BOUNDARY LAYER MEASUREMENTS USING HOT-FILM SENSORS

Harlan K. Holmes
NASA Langley Research Center
Hampton, Virginia 23665

Debra L. Carraway
Old Dominion University Research Foundation
Norfolk, Virginia 23508

SUMMARY

Measurements in the aerodynamic boundary layer using heat transfer, hot-film sensors are receiving a significant amount of effort at the Langley Research Center. A description of the basic sensor, the signal conditioning employed, and several manifestations of the sensor are given. Results of a flow reversal sensor development are presented, and future work areas are outlined.

INTRODUCTION

Aerodynamic viscous drag is the focus of an intensifying research and development effort at the Langley Research Center. The objectives of this research are to identify and quantify the origins of that drag and to implement means for its reduction whether by profile modifications or through surface treatments. Providing the aerodynamicist with a diversity of sensors and supporting electronics to perform these studies is also receiving a significantly increased development effort, particularly within the Instrument Research Division (IRD) at Langley. Past developments have resulted in a miniaturized, mechanical force balance-type skin-friction sensor which has been used in both supersonic and cryogenic flows, and an improved design is now being readied for use in the National Transonic Facility (NTF). A high sensitivity design is being constructed for use in a low speed, quiet tunnel, and units are being fabricated for an upcoming flight test program. More recently, a major effort into the development and understanding of hot-film, heat transfer sensors has begun.

Figure 1 is a conceptualization of several boundary layer sensors under development by the Instrument Research Division. Extensive development of mechanical, force balance skin-friction sensors has been completed with numerous designs having been built and tested. Devices have been fabricated of several different materials, and many have been tested at cryogenic temperatures. These units operate on a closed-loop servo principle where the current to restore the sensing element to its null position is a measure of the aerodynamic friction on the surface. A two-dimensional sensor utilizing the same concepts is now in design. The fiber optic sensor, conceptually illustrated, is expected to provide an amplitude variation in response to surface shear forces and is being pursued under a university grant. Polyvinylidine fluoride is a thin (0.0005" - 0.015") piezoelectric copolymer sheet which has the interesting property of providing voltages as a result of surface pressure fluctuations. Illustrated is a concept for a surface dynamic

pressure sensor array which will be pursued in a future program. The remaining items, the thermal skin-friction sensor; the flow reversal sensor; the crossflow sensor; and a multi-element transition sensor, will be discussed in more detail in following sections.

SYMBOLS

A	Area, cm^2
Q_a	Heat transfer by forced convection, Btu/sec
Q_c	Heat transfer by conduction to the substrate, Btu/sec
Q_i	Joulean heat input, Btu/sec
Q_r	Heat transfer by radiation to the surroundings, Btu/sec
Q_s	Heat transfer to the substrate, Btu/sec
R_f	Resistance of the film at temperature, T_f, ohms
R_o	Resistance at a reference temperature, T, ohms
$R_{()}$	Resistance as designated by the subscript, ohms
$T_{()}$	Absolute temperature, generally defined with a subscript, ^oC
h	Convective heat transfer coefficient, $Btu/m^2\text{-sec-}^oC\text{-cm}$
I	Current
k	Thermal heat transfer coefficient, $Btu/m^2\text{-sec-}^oC\text{-cm}$
ℓ	Length dimension, cm
α	Temperature coefficient of resistance, $ohm/ohm\text{-}^oC$
ε	Emissivity of the foil sensor
σ_{SB}	Stefan Boltzmann constant, 567×10^{-8} $W/m^2\text{-}^oC^4$
ρ	Coefficient of resistivity, ohm-cm

HOT-FILM SENSOR

Figure 2 is a conceptual representation of a typical metallic foil sensor mounted on a thin insulating blanket which is then bonded to the surface of a structure from which information is desired. The thinness of the insulating blanket is dictated by the requirement for a low sensor profile to prevent premature boundary layer transition. Should this not be a driving influence,

a thicker blanket having a lower conductive heat transfer can be employed. Several factors dictate the design of a sensor: the heat transfer relationship between the film and substrate, the heating capacity and controllability of the film, and other physical characteristics of both film and substrate which make them compatible with instrumentation and test surfaces. This is illustrated theoretically by performing a heat balance upon the sensor.

Heat In = Heat Out + Heat Stored (1)

Symbolically,

$$Q_i = Q_a + Q_s + Q_r + Q_{stored}$$

Where,

$Q_i = J'I^2R_f$ is the Joulean heat input

$J' = 0.484 \times 10^{-4}$ Btu/sec-W

$R_f = R_o [1 + \alpha(T_f - T_o)]$ (2)

$R_o = \rho_o \ell/A$

$Q_a = hA\Delta T$ is the heat loss due to convection

$Q_s = - kA\partial T/\partial n$ is the conductive losses to the substrate

$Q_r = \epsilon\sigma_{SB} A(T_f^4 - T_a^4)$ is the heat loss by radiation

Combining the separate terms gives

$$J'I^2 R_f = [hA\Delta T] - [kA\partial T/\partial n] + \epsilon\sigma_{SB} [A(T_f^4 - T_a^4)]$$ (3)

The terms over which some influence can be effected are as follows:

$$J'I^2 R_f = [hA\Delta T] - [kA\partial T/\partial n]$$ (4)

When the sensor is operated in a constant temperature (or resistance) system where the film is generally controlled at a temperature higher than the surroundings (overheat temperature), whatever disturbance (turbulent burst, velocity fluctuation, skin-friction variation, etc.) that arises to perturb the equilibrium temperature (resistance), translates to a change in sensor resistance. The governing electronics then forces the sensor resistance to its original controlled value. Equation (4) reveals the essence of the measurement. The last term deals with conduction to the substrate. Minimization of this term is generally desirable and is accomplished principally through selection of the material for the substrate or the temperature gradient. Since the element temperature is electronically controlled by the "overheat" (resistance) which also governs the sensitivity, the only controllable elements from which benefit can be gained are the material, which specifies the thermal conductivity, and the material thickness, which controls the temperature gradient. Since the thickness of the sensor is generally dictated by aerodynamic considerations, selection of the substrate material is the remaining variable. More discussion on the

substrate material will follow later. Looking at the first term on the right hand side of equation (4), modulation of the boundary layer profile causes changes in the temperature which are reflected in a change of film resistance. Thus, it is the task of the electronic control unit to sense this perturbation and to effect the necessary changes in current to the sensor to restore the sensor to its commanded resistance value. Before looking at the control electronics, note that selection of the film material has a profound impact on the sensitivity of the device. To see this, differentiating equation (3) with respect to the film temperature gives

$$dR_f/dT_f = \rho\alpha\ell/A \tag{5}$$

which for a given physical construction makes maximization of the $\rho\alpha$ product the feature which maximizes the device sensitivity. Table I gives information on several potential film materials.

CONDITIONING ELECTRONICS

Figure 3 describes the functional operation of the "constant temperature" anemometer system and includes a functional relationship between the system's input and output. The sensor, R_4, forms one leg of a basic wheatstone bridge. Examination of the diagram shows the circuit to be a high-gain, wide bandwidth differential measuring system with feedback to the bridge circuit. These characteristics make the circuit prone to oscillate, and care must be taken in its adjustments. The dc offset control biases the current amplifier stage into conduction, which places that stage into a more linear operating region. Knowing the resistance vs. temperature characteristics of the film sensor, one can specify an operating temperature for the film (known as overheat), which translates into a resistance at that temperature. To achieve this overheat, R_3 is increased to that value, unbalancing the bridge and causing a differential input voltage to appear at the input of the amplifier. The amplifier sends a large driving signal to the current amplifier which drives current through all resistors of the bridge, but principally through R_2 and R_4, until the heating in R_4 increases the resistance to match that of R_3 and thereby balances the bridge at the new operating point. Quite frequently, R_1 and R_3 are some multiple of the values in the other half of the bridge so that the major current flows through R_2 and the film sensor. Also shown at the left of the figure is a square (sine) wave generator which can be switched into the bridge circuit so that a signal can be injected to provide for frequency response adjustments. Care must be taken in the system design because the cable connecting the film sensor to the anemometer is also in the bridge circuit, and variations in cable or contact resistance will be indistinguishable from data. The connecting cable has inductance which introduces a reactive component in the balance equations and must be compensated for; otherwise, instabilities result. Also, R_2 must be a high-quality non-inductive temperature-insensitive resistor, or else variations in this element will also appear as data. Increasing the film resistance in order to reduce the current requirements has some restrictions. For example, use of a higher input voltage power supply can raise the differential voltage higher than the common-mode voltage limit of the input amplifier stage.

144

Also shown in figure 3 is a functional relationship of the input/output characteristic of the system. From this figure and equation (5) it should be apparent that the slope (sensitivity) is largely dependent on the sensor material. Table I lists the thermal parameters of several materials having large rho-alpha ($\rho\alpha$) products. Also apparent from this figure is the effect of heat loss to the substrate and the desirability of minimizing it. Table II lists several substrate materials and their thermal conductivity and linear expansion coefficients. Note that fused quartz and silicon dioxide have a thermal conductivity an order of magnitude greater than that for the polystyrene and polyimide families of thermoplastics. The polyimide family, more readily identified by the E. I. du Pont de Nemours and Company trademark Kapton, has many desirable properties (ref. 1):

"Polyimide precision parts can be used continuously in air at temperatures up to $500^{O}F$. The continuous operating temperature can be raised to $600^{O}F$ in an inert atmosphere or vacuum. For intermittent, short-term exposures, top temperatures appear to be in the 800° to $900^{O}F$ range.

The thermal expansion of polyimide parts is between that of metals and conventional plastics.

Tests exposing polyimide parts in liquid nitrogen indicate possible applications in cryogenic systems at $-320^{O}F$ to $-420^{O}F$. Tensile strength at $-320^{O}F$ shows a 30 percent increase above that at room temperature. Shrinkage at $-320^{O}F$, for example, is about 7 mils/in."

Figure 4 is a picture of a flight-qualified version of the circuit shown in figure 3.

THERMAL SENSORS

Figure 5 illustrates two prototype sensors, a flow reversal sensor and a 10-element crossflow sensor. Both sensors feature metallic films which are mounted on polyimide film substrates. Both sensors would be oriented as they are in the figure, with flow progressing from top to bottom. Care has been taken that the lead connections are made downstream or to the side of the sensor elements to minimize any interference with the flow. The crossflow sensor is constructed with film elements mounted on a 0.035" center-to-center spacing. This distance was determined from calculations and measurements of the average spacing between crossflow vortices. In sublimating chemicals used to visually detect this phenomenon, crossflow vortices appear as longitudinal streaks. An enlarged view of the sensor is found in figure 6. The solder pads on the terminal strip have significant height, and the connecting wire between the solder tab and the sensing element possesses a surprising amount of resistance. Figure 7 illustrates a continuous multi-element hot-film transition gage that has been developed to overcome the disadvantages of individual hot-film gages. The multi-element sensor integrates a quantity and distribution of hot-film sensing elements into a long, continuous, thin sheet. Transition data acquisition is accomplished using an electronic switching system which allows rapid switching of all sensing elements into the data recording system. The continuous thin sheet of

a particular length covers the area of interest for transition measurements beginning at the leading edge and continuing to downstream of the transition region. For example, on an airplane wing of 10 ft chord length, the gage may be as much as 7 to 8 ft in length. The leading edge of a gage mounted on the upper surface of a wing would wrap around and beneath and downstream of the wing leading edge. In this fashion, no disturbance from the film leading edge will cause turbulent wedges to disturb the hot-film sensors in the transition region. For situations where the lateral edges could cause transition, the edges may be filled and faired to correct this difficulty.

Figure 8 illustrates a completely different construction technique for building a thermal skin-friction sensor. Here, a thin foil is sandwiched between beryllium-copper sheets. This foil assembly is then bonded between two plastic cylindrical halves and trimmed. The surface is machined until resistance of the foil rises to approximately 5 ohms. At this point, leads are attached, and it is mounted in an adapter ready for tunnel test. These units have been used several times in a cryogenic test, and when compared against the mechanical force balance instruments, good agreement has been obtained.

Figure 9 is an idealized description of the fluctuating or high-frequency signals from the hot-film sensors. Within the laminar region, where there is a slow, steady heat transfer rate, the sensor requires less current input to keep the temperature constant; hence, there is a low amplitude signal. The low level of signal amplitude in the illustration indicates the presence of noise in the instrumentation system. A noise-free laminar signal would have zero amplitude. In the turbulent region, where there are large current changes with the rapid fluctuating heat transfer rates, a larger voltage change is required and results in signals of greater amplitude. Both the fluctuating and mean values of heating voltage are recorded and observed in real time using a battery-powered oscilloscope.

TUNNEL TEST OF FLOW REVERSAL SENSOR

In figure 10, the top photo is of a laminar airfoil model which was coated with oil containing carbon black and tested in IRD's small tunnel. Inspection reveals that a laminar separation bubble, which is characterized by a flow separation, reversal, and reattachment, has formed between 60 - 70% of chord. A flow reversal sensor was then mounted at this chord position along with several additional sensors mounted strategically around the model as seen in the center photograph. With this sensor configuration, a low-speed test was performed, and typical responses from the various sensors are shown along the line labeled 45 mph. At the far right is the output from the flow reversal sensor which indicates that the flow is in a reverse direction. If the velocity is increased to 185 mph, as seen at the bottom, the separation bubble moves aft because of a low Reynolds number hysteresis effect, and the sensor now shows a forward flow direction.

146

FUTURE WORK

Development work to date has revealed several areas where additional development is needed. There have been several expressed needs for large numbers of sensors both for models and full scale articles, where switching of the sensors into a limited number of signal conditioning units is required. Response time to arrive at steady state conditions needs additional definition. This may also be required in the case of the crossflow sensor where operating the gages continuously may result in thermal crosstalk because the sensors are so closely spaced. Operation in a pulse mode would reduce the average power consumed per sensor. Calibration techniques must be developed so that the system frequency response can be obtained more easily. The current trends in instrumentation are towards microprocessor involvement to provide more automatic control, monitoring, calibrating, selecting, etc.

CONCLUDING REMARKS

In this paper, several thin film, thermal sensors have been described as being applicable to boundary layer measurements with transition, flow reversal and skin-friction being the more prominent applications. A single sensor element can be used to investigate flow transition. Adding two elements, one upstream and the other downstream, allows flow reversal to be detected. Creating a spanwise array of closely spaced elements allows investigations of crossflow conditions occurring in swept wing situations. Imbedding a single filament in a low thermal conductivity plastic can be used to measure aerodynamic skin-friction if the sensor has been calibrated against a force balance type unit. All of the sensors mentioned utilize the same signal conditioning equipment which indicates that all methods have similar operational characteristics.

REFERENCES

1. Handbook of Materials and Processes for Electronics, Charles A. Harper, Editor, McGraw-Hill, Inc., 1970, pp. 1-64, 65.

2. Holmes, Bruce, J: Progress in Natural Laminar Flow Research. AIAA Paper No. 84-2222, 1984.

3. Obara, Clifford J., and Holmes, Bruce J.: Flight-Measured Laminar Boundary Layer Transition Phenomena Including Stability Theory Analysis. NASA TP 2417, 1985.

TABLE I. - POTENTIAL MATERIAL FOR SENSOR ELEMENTS

Material	Resistivity Micro-ohm-cm	Coef. of Resistivity Per Degree Celsius	Coef. of Expansion Per Degree Celsius
BALCO (1)	19.9	0.0045	0.000015
"A" Nickel	10.0	0.0048	0.000013
Platinum	10.6	0.003	0.0000088
Copper	1.73	0.0039	0.0000166
Columbium	14.2	0.0395	0.0000069
Tungsten	5.48	0.0045	0.0000046
Titanium	55.0	0.0041	0.0000085
Nichrome	105.0	0.0014	-

(1)   BALCO is a Trademark of W. B. Driver Company

TABLE II. - MATERIAL FOR INSULATION

Material	Thermal conductivity cal/cm^2-sec-^oC-cm	Coef. of Expansion Per Degree Celsius
Fused Quartz	0.0033	0.00000055
Silicon Dioxide	0.00256	-
Balsawood	0.000116	-
Polysulphone	0.000162	0.000056
Polystyrene	0.00030	0.000065
Polyester	0.000363	0.000027
Nylon 6	0.00059	0.00007
Polyimide	0.00035	-
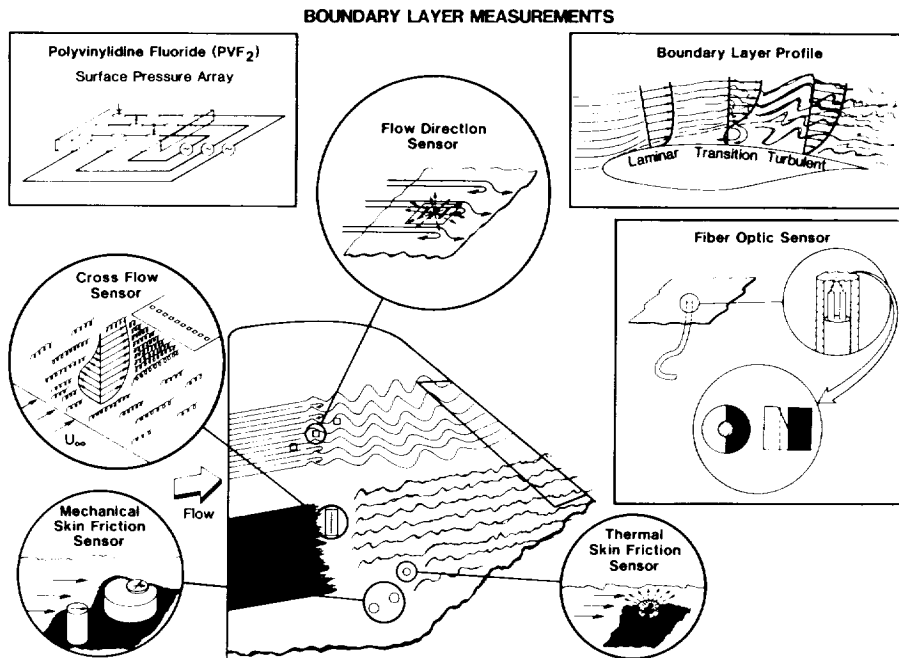
Figure 1.- Boundary layer measurement concepts.
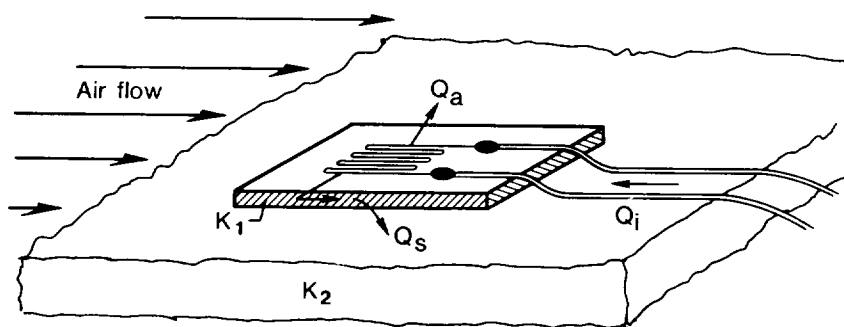
Q_i = Input electrical power (Joulean heating)

Q_a = Heat transfer by forced convection

Q_s = Heat transfer by conduction to substrate

$K_{1,2}$ = Thermal heat transfer coefficients
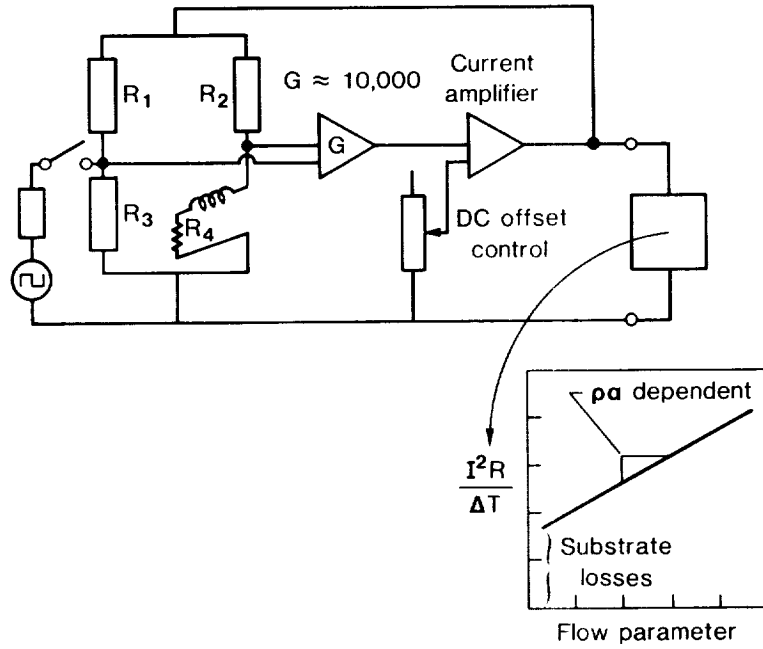
Figure 2.- Metallic foil thermal sensor.

149

Figure 3.- Anemometer functional schematic and input/output functional relationship.
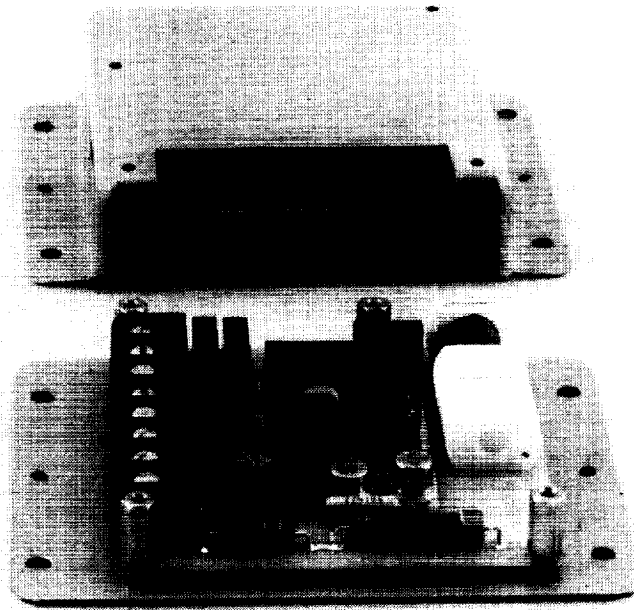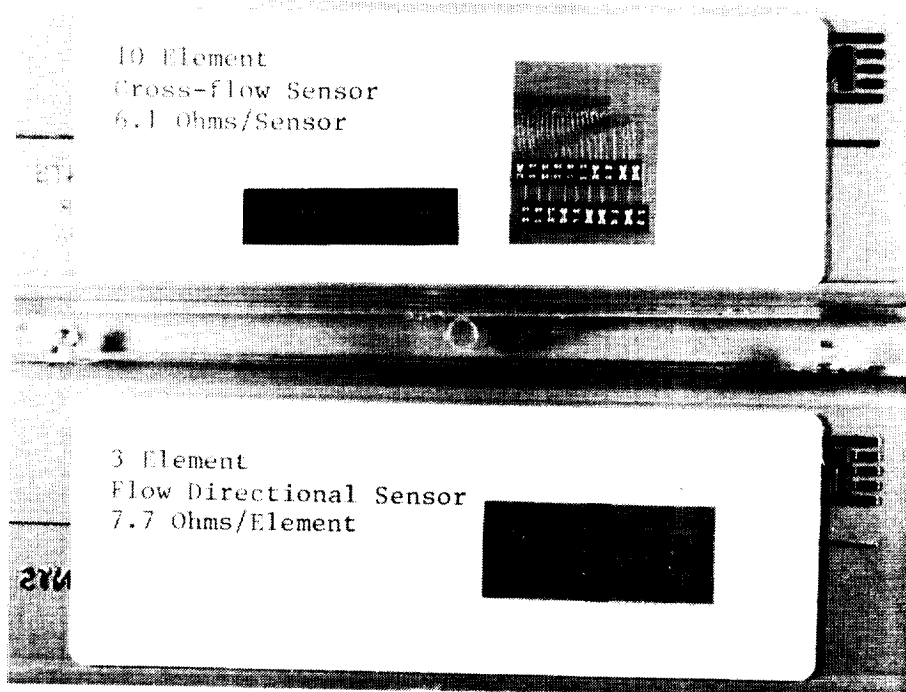
Figure 4.- Flight qualified anemometer package.

Figure 5.- Prototype flow reversal and cross-flow sensors.
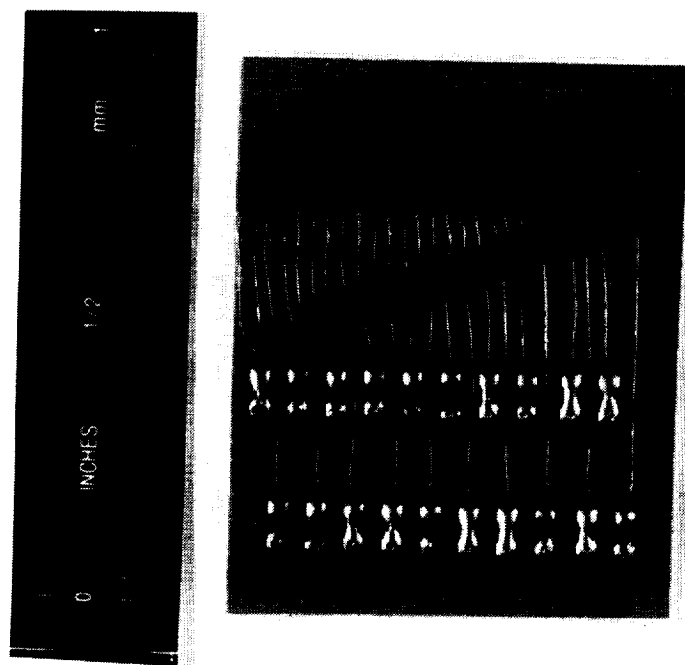
Figure 6.- Prototype cross-flow sensor.
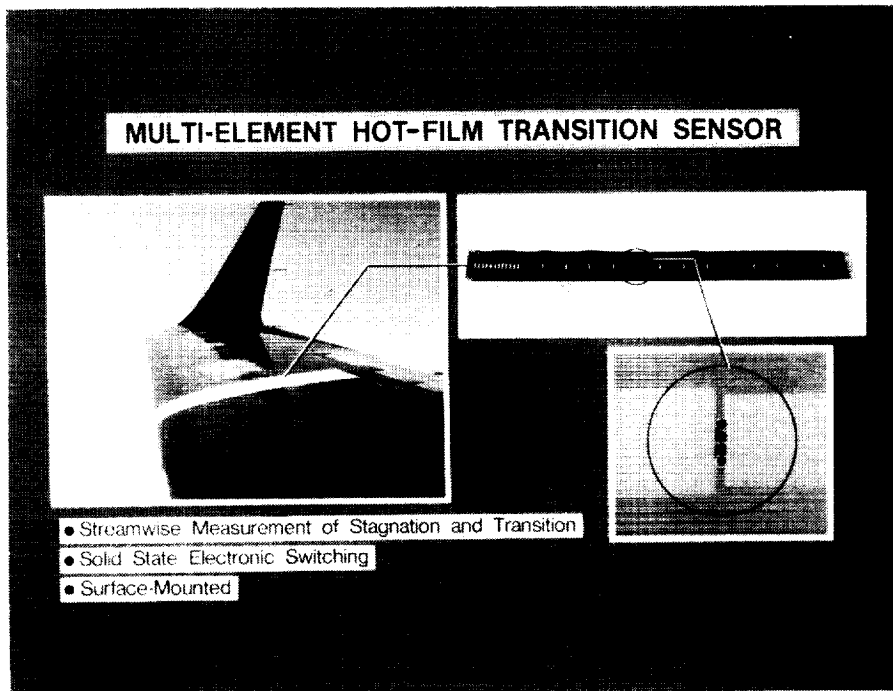
Figure 7.- Multi-element hot-film transition sensor (ref. 2).

Figure 8.- Thermal skin-friction sensor.

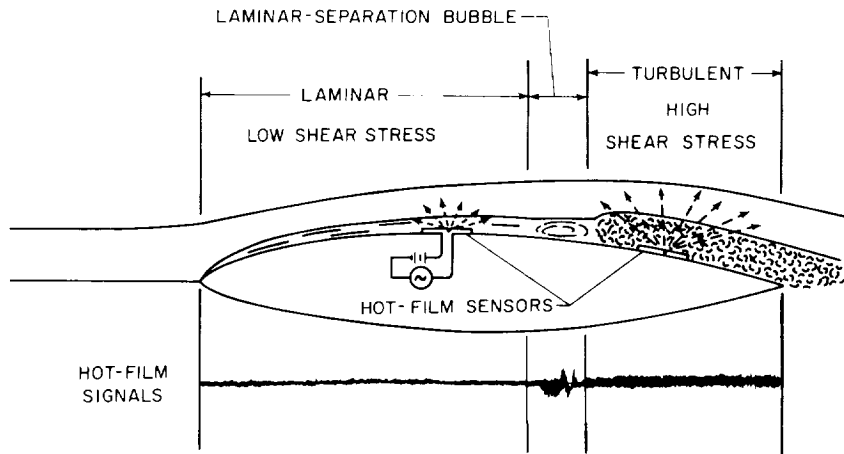## LAMINAR AND TURBULENT FLOW INDICATED
BY HOT FILMS

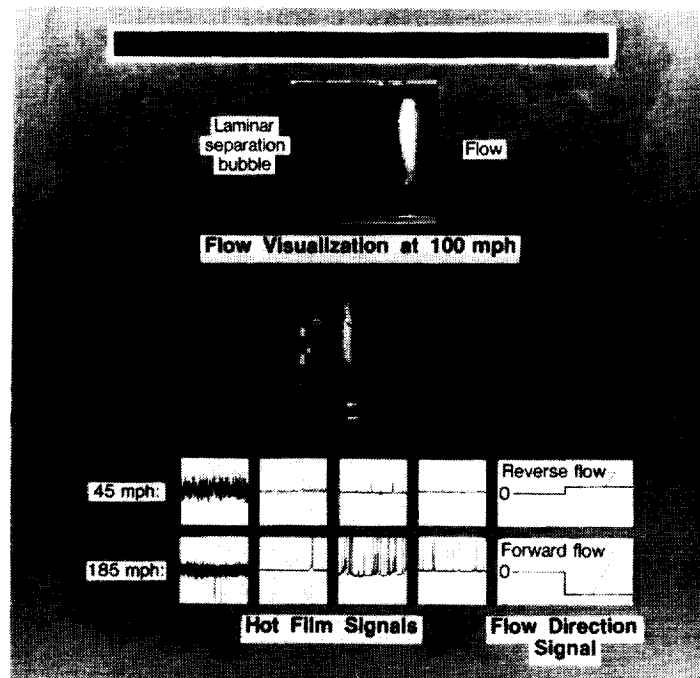Figure 9.- Hot-film signal characteristics for laminar, laminar separation, and turbulent boundary layer conditions (ref. 3).

Figure 10.- Flow reversal sensor test results.